

The electron-phonon coupling is large for localized states

Raymond Atta-Fynn,* Parthapratim Biswas,† and D. A. Drabold‡
Department of Physics and Astronomy, Ohio University, Athens, OH 45701

From density functional calculations, we show that localized states stemming from defects or topological disorder exhibit an anomalously large electron-phonon coupling. We provide a simple analysis to explain the observation and perform a detailed study on an interesting system: amorphous silicon. We compute first principles deformation potentials (by computing the sensitivity of specific electronic eigenstates to individual classical normal modes of vibration). We also probe thermal fluctuations in electronic eigenvalues by first principles thermal simulation. We find a strong correlation between a static property of the network [localization, as gauged by inverse participation ratio (IPR)] and a dynamical property (the amplitude of thermal fluctuations of electron energy eigenvalues) for localized electron states. In particular, both the electron-phonon coupling and the variance of energy eigenvalues are proportional to the IPR of the localized state. We compare the results for amorphous Si to photoemission experiments. While the computations are carried out for silicon, very similar effects have been seen in other systems with disorder.

PACS numbers: 71.23.Cq, 71.15.Mb, 71.23.An

Keywords: amorphous silicon, electron localization, electron-phonon coupling

I. INTRODUCTION

Electron states of finite spatial extent, so called “localized” states are ubiquitous in nature. Localized molecular orbitals occur in molecules and in solid state systems with disorder (this could take the form of defects, such as a dangling bond state or more subtly from topological and or chemical disorder in amorphous materials or glasses). Such localized states are also known in polymers. Surface states, as another form of defect, also are often spatially compact. The study of localization in its own right has been an important and active subfield of condensed matter theory since the fifties.

Another physical quantity of key importance is the electron-phonon (e-p) coupling, the interaction term connecting the electronic and lattice systems. Perhaps most spectacularly, the e-p coupling is the origin of superconductivity as expressed in BCS theory¹. Phillips² has shown that large e-p couplings in the cuprate superconductors can lead to a successful model of high T_c superconductivity³ within the framework of conventional BCS superconductivity. The e-p coupling is also the mediator of all light-induced structural changes in materials. In amorphous silicon the greatest outstanding problem of the material, the Staebler-Wronski effect⁴, depends critically upon the electron-lattice interaction. A zoo of analogous effects is studied in glasses; perhaps the most important example is reversible photo-amorphization and photo-crystallization used in the GeSbTe phase-change materials used in current writable CD and DVD technology.

Previous thermal simulations with Bohn-Oppenheimer dynamics have indicated that there exists a large electron-phonon coupling for the localized states in the band tails and in the optical gap^{5,6}. Earlier works on chalcogenide glasses by Cobb and Drabold⁷ have emphasized a strong correlation between the thermal fluctuations as gauged by root mean square (RMS) vari-

ation in the LDA eigenvalues and wave function localization of a gap or tail state (measured by inverse participation ratio⁸, a simple measure of localization). Drabold and Fedders⁹ have also shown that localized eigenvectors may fluctuate dramatically even at room temperature. Recently, Li and Drabold relaxed the adiabatic (Born-Oppenheimer) approximation to track the time-development of electron packets scattered by lattice vibrations⁶. In this paper, we examine the electron phonon coupling and provide a heuristic analysis of the e-p coupling for localized electron states. We explore the e-p coupling in some detail for a particular model system (amorphous silicon) which provides us with a convenient variety of localized, partly localized “bandtail” and extended states. We compute deformation potential (which measures the response of a selected electron state to a particular phonon), and also track thermally-induced fluctuations of electronic eigenvalues. We find that localized states always exhibit a large e-p coupling. Our computations are carried out using a first principles molecular dynamics code SIESTA, and the eigenvalues and states that we study are from the Kohn-Sham equations with a rich local orbital basis. A rationale for the study of the Kohn-Sham states is given elsewhere¹⁰. We emphasize that the results that we give are qualitatively general – not just an artifact of studying a disordered phase of silicon (we have, for example, seen exactly the same effects in various binary glasses which exhibit very different topological and chemical disorder).

II. THEORY

To establish a connection between electron-phonon coupling and wave function localization for the electrons, we consider an electronic eigenvalue λ_n near the band gap of a-Si. The sensitivity of λ_n due to an arbitrary small displacement of an atom (possibly thermally in-

duced) can be estimated using the Hellmann-Feynman theorem¹¹,

$$\frac{\partial \lambda_n}{\partial \mathbf{R}_\alpha} = \langle \psi_n | \frac{\partial \mathbf{H}}{\partial \mathbf{R}_\alpha} | \psi_n \rangle.$$

Here we have assumed that the basis functions are fixed and $|\psi_n\rangle$ are the eigenvectors of the Hamiltonian \mathbf{H} . For small lattice distortion $\{\delta \mathbf{R}_\alpha\}$, the corresponding change in $\delta \lambda_n$ is,

$$\delta \lambda_n \approx \sum_{\alpha=1}^{3N} \langle \psi_n | \frac{\partial \mathbf{H}}{\partial \mathbf{R}_\alpha} | \psi_n \rangle \delta \mathbf{R}_\alpha \quad (1)$$

where N is the total number of atoms in the model. If the displacement $\delta \mathbf{R}_\alpha(t)$ arises from classical vibrations, one can write¹²,

$$\delta \mathbf{R}_\alpha(t) = \sum_{\omega=1}^{3N} A(T, \omega) \cos(\omega t + \phi_\omega) \chi_\alpha(\omega), \quad (2)$$

where ω indexes the normal mode frequencies, $A(T, \omega)$ is the temperature dependent amplitude of the mode with frequency ω , ϕ_ω is an arbitrary phase, $\chi_\alpha(\omega)$ is a normal

mode with frequency ω and vibrational displacement index α . Using the temperature dependent squared amplitude $A^2 = 3k_B T / M\omega^2$, the trajectory (long time) average of $\delta \lambda_n^2$ can be written (using Eq. 1 and 2) as,

$$\langle \delta \lambda_n^2 \rangle = \lim_{\tau \rightarrow \infty} \frac{1}{\tau} \int_0^\tau dt \delta \lambda_n^2(t) \approx \left(\frac{3k_B T}{2M} \right) \sum_{\omega=1}^{3N} \frac{\Xi_n^2(\omega)}{\omega^2}, \quad (3)$$

where the electron-phonon coupling $\Xi_n(\omega)$ is given by,

$$\Xi_n(\omega) = \sum_{\alpha=1}^{3N} \langle \psi_n | \frac{\partial \mathbf{H}}{\partial \mathbf{R}_\alpha} | \psi_n \rangle \chi_\alpha(\omega). \quad (4)$$

One can infer from Eq. 3 that thermally induced fluctuation in the energy eigenvalues is a consequence of electron-phonon coupling. Note that for a given electronic eigenvalue, the contribution to the coupling comes from the entire vibrational spectrum involving all the atoms in the systems. Since the normalized eigenstate can be written as $|\psi_n\rangle = \sum_i a_{ni} |i\rangle$ where $|i\rangle$ are the basis orbitals, it follows from Eq. 4 that,

$$\begin{aligned} \Xi_n^2(\omega) &= \sum_{\alpha, \beta, i, j, k, l} a_{ni}^* a_{nj} a_{nk}^* a_{nl} \langle i | \frac{\partial \mathbf{H}}{\partial \mathbf{R}_\alpha} | j \rangle \langle k | \frac{\partial \mathbf{H}}{\partial \mathbf{R}_\beta} | l \rangle \chi_\alpha(\omega) \chi_\beta(\omega) \\ &= \sum_{i, \alpha} |a_{ni}|^4 \left[\langle i | \frac{\partial \mathbf{H}}{\partial \mathbf{R}_\alpha} | i \rangle \right]^2 \chi_\alpha^2(\omega) + \sum'_{ijkl\alpha\beta} a_{ni}^* a_{nj} a_{nk}^* a_{nl} \langle i | \frac{\partial \mathbf{H}}{\partial \mathbf{R}_\alpha} | j \rangle \langle k | \frac{\partial \mathbf{H}}{\partial \mathbf{R}_\beta} | l \rangle \chi_\alpha(\omega) \chi_\beta(\omega) \end{aligned} \quad (5)$$

The first term in the second line of Eq. 5 is positive definite (diagonal) while the second one, the off-diagonal term (indicated by the prime), is not of a single sign. In the event that only a few a_{ni} dominate (the case for localized states), then the leading contribution to the electron-phonon coupling originates largely from the diagonal term. The addition of a large number of terms of mixed sign and small magnitude leads to cancellations in the off-diagonal term leaving behind a small contribution to electron-phonon coupling. By comparing to direct calculations with the full Eq. 5, we show that dropping the second term appears to be reasonable for well-localized electron states. The approximate ‘‘diagonal’’ electron-phonon coupling can be written as,

$$\begin{aligned} \Xi_n^2(\omega) &\approx \sum_{\alpha=1}^{3N} \sum_{i=1}^{N_b} |a_{ni}|^4 \left[\langle i | \frac{\partial \mathbf{H}}{\partial \mathbf{R}_\alpha} | i \rangle \right]^2 \chi_\alpha^2(\omega) \\ &= \sum_{\alpha=1}^{3N} \sum_{i=1}^{N_b} q_{ni}^2 \left[\langle i | \frac{\partial \mathbf{H}}{\partial \mathbf{R}_\alpha} | i \rangle \right]^2 \chi_\alpha^2(\omega) \end{aligned} \quad (6)$$

where N_b is the number of basis orbitals and $q_{ni} = |a_{ni}|^2$ is the charge sitting on the i th orbital for a given normalized eigenstate $|\psi_n\rangle$. The degree of wave function localization can be measured by defining inverse participation ratio \mathcal{I} for the eigenstates $|\psi_n\rangle$,

$$\mathcal{I}(n) = \sum_{i=1}^{N_b} q_{ni}^2. \quad (7)$$

Equation 6 leads to an approximate but analytic connection between \mathcal{I} and electron-phonon coupling. Since \mathcal{I} is large for localized states, one expects $\Xi_n(\omega)$ (and therefore $\langle \delta \lambda_n^2 \rangle$) to be large for a localized state. If we further assume that $\gamma^2(\omega, i) = \sum_{\alpha=1}^{3N} \left[\langle i | \frac{\partial \mathbf{H}}{\partial \mathbf{R}_\alpha} | i \rangle \right]^2 \chi_\alpha^2(\omega)$ is weakly dependent upon site/orbital index i , then

$$\Xi_n^2(\omega) \sim \mathcal{I}_n \times f(\omega), \quad (8)$$

where $f(\omega)$ is defined from γ^2 and Eq. 6. In this ‘‘separable’’ approximation, it is also the case that $\langle \delta \lambda_n^2 \rangle \propto \mathcal{I}_n$.

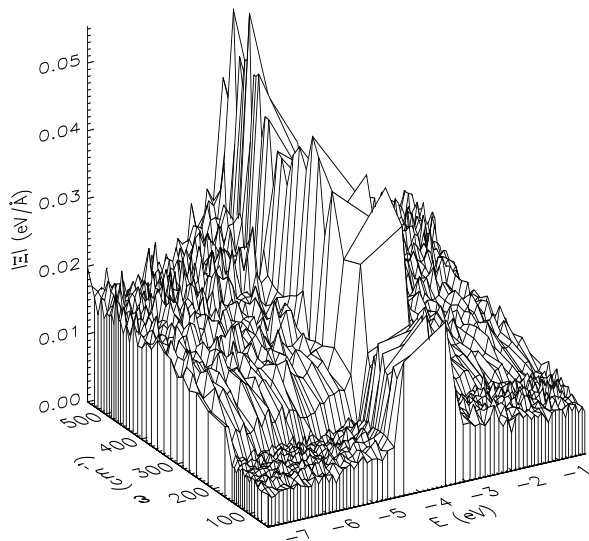


FIG. 1: Electron-phonon coupling surface plot for a 216-atom model of *a*-Si. The absolute value of electron-phonon coupling $|\Xi|$ (cf. Eq. 4) is plotted as a function of phonon frequency ω and energy eigenvalues near the gap. The largest value of $|\Xi|$ in the plot corresponds to the eigenvalue for HOMO, which is the most localized state in the spectrum.

III. METHOD

The model of *a*-Si we have used in our calculations was generated by Barkema and Mousseau¹³ using an improved version of the Wooten, Winer and Weaire (WWW) algorithm¹⁴. The details of the construction was reported in Ref. 13. The model consists of 216 atoms of Si packed inside a cubic box of length 16.282Å and has two 3-fold coordinated atoms. The average bond angle is 109.5° with a root mean square deviation of 11.0°. The density functional calculations were performed within the local density approximation (LDA) using the first principles code SIESTA^{15,16,17}. We have used a non self-consistent version of density functional theory based on the linearization of the Kohn-Sham equation by Harris functional approximation¹⁸ along with the parameterization of Perdew and Zunger¹⁹ for the exchange-correlation functional. The choice of an appropriate basis is found to be very important and has been discussed at length in a recent communication¹⁰. While the minimal basis consisting of one *s* and three *p* electrons can adequately describe the electronic structure of amorphous silicon in general, there is some concern about the applicability of these minimal basis in describing deeply localized and low lying excited states in the conduction bands accurately. We have therefore employed a larger single- ζ basis with polarization (*d*) orbitals (SZP)^{20,21} in the present work.

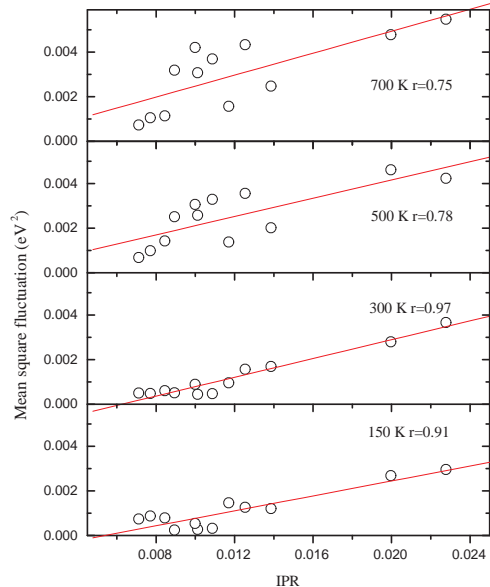


FIG. 2: (Color online) Mean square fluctuations of electronic eigenvalues versus inverse participation ratio plot at different temperature. The fluctuations at temperature 150K and 300K are found to be linearly correlated with the participation ratio for the corresponding eigenstates as predicted in section II. The correlation coefficient (r) for different temperature is indicated in the plot.

Throughout the calculation we have used only the Γ point to sample the Brillouin zone.

Starting with a fully relaxed configuration, we construct the dynamical matrix elements by successively displacing each atom in the supercell along three orthogonal directions (*x*, *y* and *z*) by 0.01Å and computing the forces for each configuration. Within the harmonic approximation, the spring constant associated with each atom and direction can be written as a second derivative of the total energy with respect to the displacement of the atom in that direction. We have checked the convergence of both the matrix elements by using a different set of values for atomic displacement and used a value of 0.01Å in our calculations. $\partial\lambda/\partial\mathbf{R}_\alpha$ was obtained by finite differences from the dynamical matrix calculations. The calculation does not need any extra effort beyond that of forming the dynamical matrix.

To explore the validity of our analysis and to elucidate the connection between the localization (IPR) (\mathcal{I}) of electronic eigenstates and fluctuation of the conjugate eigenvalues, we performed thermal MD simulations at constant temperatures using a Noé-Hoover thermostat. The simulations were performed at temperatures 150K, 300K, 500K and 700K with a time step of 2.5fs for a total period of 2.5ps. For a given temperature, the mean square fluctuations were computed by tracking the eigenvalues at each time step and averaging over the total time

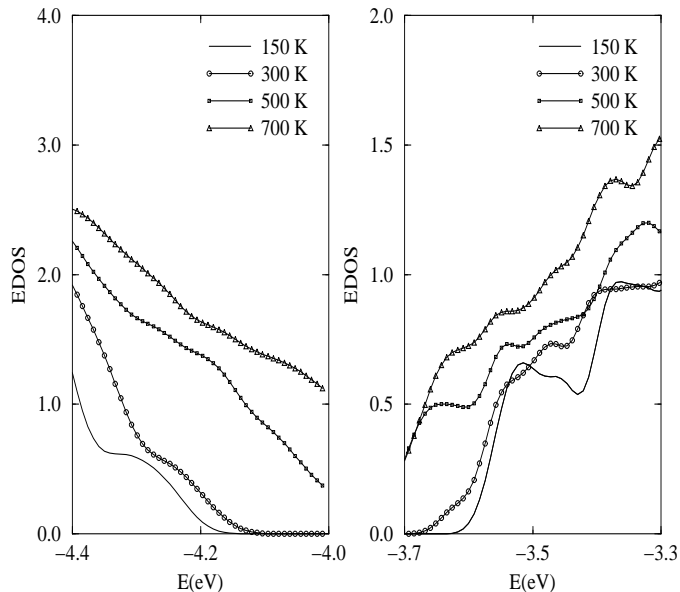


FIG. 3: The average electronic density of band tails states for four different temperature $T = 150\text{K}$, 300K , 500K and 700K . Note that the conduction band tails (right) near the Fermi level (which is between the two tails) are more sensitive to thermal disorder than the valence band tails (left) providing a qualitative agreement with experimental result in Ref. 25.

of simulation excepting the first few hundred time steps to ensure equilibration. The mean square fluctuation (\mathcal{R}) for an energy eigenvalue $\lambda_n(t)$ is defined as :

$$\mathcal{R}_n = \langle (\lambda_n(t) - \langle \lambda_n \rangle)^2 \rangle, \quad (9)$$

where $\langle \rangle$ denotes the average over time. We study the fluctuations of $\{\lambda_n(t)\}$ by plotting against time at a given temperature and compare it with the \mathcal{I} obtained for the corresponding eigenvalues. For illustrations of such adiabatic evolution of Kohn-Sham eigenvalues, see Ref. 9.

IV. RESULTS

In Fig. 1, we have plotted the electron-phonon coupling for the states near the band gap obtained directly from Eq. 4. It is clear from the figure that the e-p coupling is large only in the vicinity of conduction and valence band tails. The largest e-p coupling in the plot corresponds to the highest occupied molecular orbital (HOMO) in the optical frequency regime around 415 cm^{-1} . The lowest occupied molecular orbital (LUMO) also has a large feature around the same frequency. A Mulliken charge analysis and inverse participation ratio calculation of the electronic eigenfunctions have shown that both these two states – the HOMO and LUMO are highly localized and

are centered around the dangling bonds present in the model. On moving further from the band tails in either direction along the energy axis, the e-p coupling drops quickly and the surface becomes featureless for a given eigenvalue. This behavior of e-p coupling can be understood from the arguments presented in section II where we have shown that the e-p coupling for localized states is directly proportional to the inverse participation ratio. For a localized state, therefore, the large value of electron-phonon coupling can be attributed to the large value of inverse participation ratio associated with that state. Since HOMO and LUMO are the two most localized states in the spectrum, the e-p coupling is large for these states and as we move toward the tail states, the coupling decreases. It is important to note that the plot in the Fig.1 has been obtained from Eq. 4 without making any approximation and is exact inasmuch as the matrix elements obtained from the density functional Hamiltonian are correct. This observation supports our assumptions that the dominant contribution to e-p coupling comes from the diagonal term in Eq. 5 and that $\gamma^2(\omega, i)$ is weakly dependent upon site/orbital index i and also indicates from direct simulation there exists a linear relationship between mean square fluctuation of electronic eigenvalues and the corresponding inverse participation ratio for localized states.

In order to justify our arguments further presented in section II, we now give a look at the mean square fluctuation of energy eigenvalues. As outlined in section III, we have computed the mean square fluctuations at four different temperature (150K , 300K , 500K and 700K) from MD runs over a period of 2.5ps and plotted in the Fig. 2. The fluctuation obtained this way provides a dynamical characteristic of the band tails states and is compared with a static property, the inverse participation ratio of the same states. A simple linear fit reveals a strong correlation between the eigenvalue fluctuation and the corresponding inverse participation ratio for the states. The correlation is found to be as high as ≈ 0.95 for $T=150\text{K}$ and 300K and falls to ≈ 0.8 at high temperature. The value of the correlation coefficient for different temperature is indicated in the Fig. 2. Once again, we see that the result is in accordance with our prediction in section II and provides a simple physical picture for having a large electron-phonon coupling for the localized states.

In Fig. 3, we have plotted the time averaged electronic density of states for four different temperature in order to study the effect of thermal disorder on the tail states. It is quite clear from the figure that the effect of thermal broadening is quite significant on both sides of the gap. Photoelectron spectroscopic studies on *a*-Si:H by Aljishi et al.²² have shown that the conduction tail is indeed more susceptible to thermal disorder than the valence tail. The temperature dependence can be conveniently expressed by introducing a characteristic energy E_0 and fitting the electronic density of states to $\rho(E) \approx \exp(|E - E_f|/E_0(T))$. Aljishi et al. expressed the temperature dependence of the tail states by the slope

of the $E_o(T)$ vs. T plot and obtained a smaller value for the conduction band tail. We have observed a qualitative agreement of our results with experiment. The key observation that one should note from Fig. 3 is the following: the shape of the tail in the conduction band rapidly changes as the temperature rises from 150K to 700K. The corresponding change in the valence tail for the same range of energy (0.4eV) is however much less and is rather smooth compared to the conduction tail. Since the localized defect states (coming from the two dangling bonds) have been removed before plotting, this observation qualitatively suggests that the conduction tail states are more susceptible to lattice motion. It is tempting to attempt to estimate decay parameters for a direct comparison to experiment²², but the sparse sampling of tail states for this 216-atom model makes this a dangerous exercise. The basic features do appear to be represented in our study, however.

V. CONCLUSION

Using accurate methods and a reasonable model of a-Si, we showed that there is 1) a large e-p coupling

for localized states, 2) a significant correlation between thermal fluctuation of electron energy eigenvalues conjugate to localized states and the IPR of the model at $T=0$, 3) We find qualitative agreement with photoemission experiments²², 4) we provide a simple analytic argument for the origin of these effects. Identical experience with models of other amorphous materials has convinced us that the results are correct in at least a qualitative way for binary glasses and amorphous materials, and perhaps other systems beside.

Acknowledgments

We thank the National Science Foundation for support under grants DMR-0205858 and DMR-0310933. We thank Dr. J. C. Phillips for helpful conversations and pointing out the larger significance of the results. We thank Normand Mousseau for sending us the model of amorphous silicon used in this calculation.

* Electronic address: attafynn@phy.ohiou.edu

† Electronic address: biswas@phy.ohiou.edu

‡ Electronic address: drabold@ohio.edu

¹ J. Bardeen, L. N. Cooper, J. R. Schrieffer, Phys. Rev. **108**, 1175 (1957).

² J. C. Phillips, Phys. Rev. Lett. **72** 3863 (1994); *ibid.* **59** 1856 (1987).

³ J. G. Bednorz and K. A. Mueller, Z. Phys. B **64**, 189 (1986).

⁴ D. Staebler and C. R. Wronski, Appl. Phys. Lett. **31**, 292 (1977).

⁵ D. A. Drabold and Jun Li, *Amorphous and heterogeneous silicon based films*, Materials Research Society Proceedings. Vol. **715**, 2002.

⁶ Jun Li and D. A. Drabold, Phys. Rev. B **68** 033103 (2003).

⁷ M. Cobb and D. A. Drabold, Phys. Rev. B **56**, 3054 (1997).

⁸ The IPR (I) is in fact a useful but *ad hoc* measure of localization (a more fundamental gauge is the information entropy). From a practical point of view however, the IPR usually gives a result qualitatively similar to the entropy. See D. A. Drabold, P. Biswas, T. DeNyago and R. Atta-Fynn, in *Non-crystalline Materials for Optoelectronics*, M. Popescu and G. Lucovsky Ed., INOE, Bucharest, 2004; cond-mat/0312607.

⁹ D. A. Drabold, P. A. Fedders, Stefan Klemm and O. F. Sankey, Phys. Rev. Lett. **67**, 2179 (1991); D. A. Drabold and P. A. Fedders, Phys. Rev. B **60**, R721, (1999); D. A. Drabold, J. Non-Crys. Sol. **266**, 211 (2000).

¹⁰ R. Atta-Fynn, P. Biswas, P. Ordejón and D. A. Drabold, Phys. Rev. B (In press); cond-mat/032333

¹¹ R. P. Feynman, Phys. Rev. **56**, 340 (1939)

¹² Here we have only considered the Γ point in our calculations which corresponds to $\vec{k}=0$.

¹³ G. T. Barkema and N. Mousseau, Phys. Rev. B **62**, 4985 (2000).

¹⁴ F. Wooten, K. Winer, and D. Weaire, Phys. Rev. Lett. **54**, 1392 (1985).

¹⁵ P. Ordejón, E. Artacho and J. M. Soler, Phys. Rev. B **53**, 10441, (1996).

¹⁶ D. Sánchez-Portal, P. Ordejón, E. Artacho and J. M. Soler, Int. J. Quantum Chem. **65**, 453 (1997)

¹⁷ J. M. Soler, E. Artacho, J. D. Gale, A. García, J. Junquera, P. Ordejón, and D. Sanchez-Portal, J. Phys. Cond. Matter. **14**, 2745 (2002).

¹⁸ J. Harris, Phys. Rev. B **31**, 1770 (1985).

¹⁹ J. P. Perdew and A. Zunger, Phys. Rev. B **23**, 5048 (1981).

²⁰ O. F. Sankey and D. J. Niklewski, Phys. Rev. B **40**, 3979 (1989).

²¹ For amorphous silicon single- ζ polarized basis consists of one s and three p and five d valence electrons. For details on the generation of the basis orbitals, see E. Artacho, D. Sánchez-Portal, P. Ordejón, A. García, and J. M. Soler, phys. stat. sol. (b) **215**, 809 (1999).

²² S. Aljishi, J. D. Cohen, S. Jin and L. Ley, Phys. Rev. Lett. **64**, 2811 (1990)